MATHEMATICAL BIOSCIENCES
AND ENGINEERING
Volume **7**, Number **3**, July **2010**

doi:10.3934/mbe.2010.7.479

pp. **479–504**

IMPACT DYNAMICS IN BIPED LOCOMOTION ANALYSIS: TWO MODELLING AND IMPLEMENTATION APPROACHES

Khalid Addi[1]

University of La Réunion
Analyse et Ingénierie Mathématique AIM/LIM EA 2525
Parc Technologique Universitaire, Bâtiment 2, 2 rue Joseph Wetzell
97490 Sainte-Clotilde, France

Aleksandar D. Rodić

Robotics department, Mihajlo Pupin Institute, University of Belgrade
Zvezdara, Volgina 15, 11060 Belgrade, Serbia

(Communicated by Stefano Boccaletti)

Abstract. Stability during the biped locomotion and especially humanoid robots walking is a big challenge in robotics modelling. This paper compares the classical and novel methodologies of modelling and algorithmic implementation of the impact/contact dynamics that occurs during a biped motion. Thus, after establishing the free biped locomotion system model, a formulation using variational inequalities theory via a Linear Complementarity Problem then an impedance model are explicitly developed. Results of the numerical simulations are compared to the experimental measurements then the both approaches are discussed.

1. **Introduction.** Strong demands of precise description and accurate mathematical modeling of human locomotion in medicine, biomechanics, sport, humanoid and rehabilitation robotics, etc., are serious challenge to the scientists. Testing and analysis of the physical abilities of the handicapped and/or injured patients or aged people (for the purpose of physiotherapy and medical recover) is sometimes dangerous and painful and can be very expensive, too. To generate new technics of the exercises or to improve existing ones in sport demands the general model of human locomotion, valid for different human postures. To design the optimal structure of a biped mechanism as well as to control humanoid robots, researchers need very accurate kinematic and dynamic models of biped locomotion mechanisms. Also, accurate model of biped locomotion is necessary in rehabilitation robotics to ensure to the designer to adopt the active prothesis or equipment to the patient necessities. To get a clear insight into the system (biological or technical) behavior in many locomotion manoeuvres under the same or different test conditions, the advance mathematical models have to be derived.

2000 *Mathematics Subject Classification.* 90C33, 70E18, 37M05.

Key words and phrases. Nonsmooth dynamical systems, impact dynamics, unilateral contact, Linear Complementarity Problem, humanoid robots, impedance model.

Both authors are supported by the PHC Pavle Savic program (17699 VK).

[1]corresponding author

Humanoids, being the future of robotic science, are becoming more and more human-like in all aspects of their functioning. Thus, it is generally accepted that their shape and motion should be based on biomechanical principles. Because of the complexity and high requirements imposed on such robots, their control system has to utilize the dynamic model. So, the control, the design, and the simulation, strongly require general dynamic models that will make humanoid robots capable of handling the increasing diversity of expected tasks [1, 2].

Biped locomotion, in the sense of gait stability and maintenance of dynamic balance, represents one of the most complex known natural motions. Anthropomorphic locomotion is performed by a synergy of large number of body muscles. Performances of biped gait differs from person to person, depending on different factors such as: physical and physiological capabilities and some pathologic conditions but sometimes also on psychological condition of the person, etc.

Human motion, where the locomotion system is in contact with the ground support (walking, climbing the stairs, running, gymnastic exercise, etc.) or some other mobile supporting object is in research focus of this contribution. The authors are well aware of the extreme complexity of the problem of modeling biological systems, which stems from the complexity of the mechanical structure and actuation. The fact that the control of biological system is a still insufficiently studied area, contributes greatly to the significance of the problem.

The stability of the humanoid robot depends of the precision of the dynamics approximation. Indeed, in the instant when the foot of the swinging leg comes into contact with the ground, a large impact force can be generated. Active control of such impact force would require robot's controllers and actuators to have very wide bandwidth and be capable of generating a large instantaneous power. It is not realistic to have controllers with a wide bandwidth and huge powerful actuators, which add more weight to the biped robot.

This paper deals especially with impact dynamics and the frictional contact modelling of the biped feet with the ground in order to increase the dynamics approximation allowing better stability. Authors developed a new and more precise frictional impact/contact model alternative to the traditional models usually implemented by the robotics community among them the impedance model.This approach yields a Linear Complementarity Problem formulation (LCP) model. The LCP formulation belongs to the family of the variational inequalities theory [3, 4, 5, 6]. Besides the accuracy, implementing models have other requirements namely computation speed. This paper develops mainly a comparison of the two cited approaches showing their different properties and their applicability range.

The paper starts with the biped locomotion modelling then presents the two contact models and the results of the numerical simulations. The last part is devoted to the comparison of the different approaches

2. **Modeling of biped locomotion.** To move, human body uses more than 600 muscles and 300 degrees of freedom (DOFs) [7]. Let us consider the biped robotic system of the anthropomorphic structure illustrated in Figure 2. Let the joints of the system be such to allow n independent motions. Let these joint motions be described by joint angles forming the vector of the generalized coordinates $q = [q_1 \dots q_n]^T$. In this paper, a biped locomotion mechanism of the anthropomorphic structure will be considered as a mechanical representative of human body. In that sense, an articulated system, consisting of the basic kinematic chain and four side

branch chains, as shown in Figure 2, is considered as a biped mechanism. In a mechanical sense, it represents a multi-body, large-scale dynamic system with a variable structure. Concerning the kinematic structure, the torso is assumed to be the basic link or just the basis of the mechanism. The arms and the legs represent the corresponding branches known in robotics as lateral kinematic chains. Let us consider the mechanical system of the anthropomorphic structure illustrated in Figure 2. It represents a complex, branched kinematic chain with N mechanical

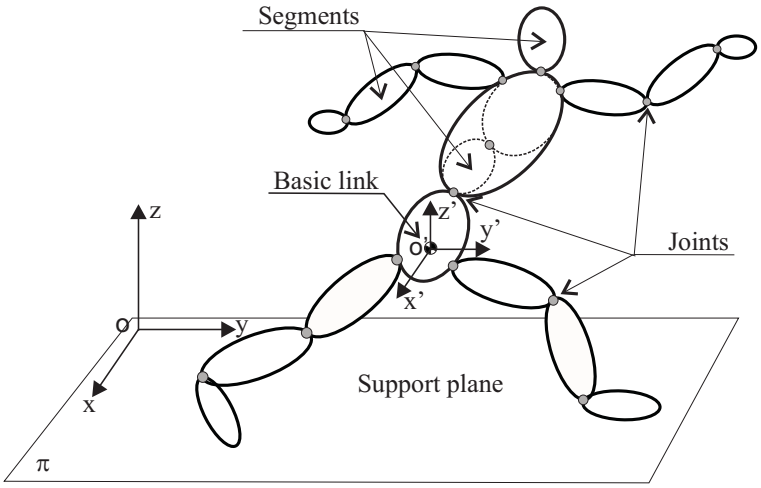

FIGURE 1. Complex kinematic structure of a biped locomotion mechanism - branched kinematic chain of the anthropomorphic structure

degrees of freedom (DOFs). Its motion is defined in the fixed coordinate system attached to the plane of motion. Position of the mechanism in the free space is determined by the relative position of the mobile coordinate system $O'x'y'z'$ with respect to the reference coordinate system $Oxyz$ (Figure 2a). The mobile coordinate system $O'x'y'z'$ is attached to the mass center of the lower trunk (the hip link) that is assumed to be the basic link, i.e. the basis of the robot. Simultaneously with the displacement of the basic link, the rotations of the biped links at the mechanism's joints take place. Thus the entire mechanism, keeping its lump mass constant, changes its inertial properties due to the motion of biped links at the joints of the arms, legs and trunk. Besides, due to the motion of the mechanism as well as due to the influence of the external disturbances acting upon the system or carrying the payload the contact forces and contact moments arise at the particular points of the biped mechanism. Let the joints of the system be such to allow n independent motions. Let these joint motions be described by joint angles forming the vector of the generalized coordinates $q = [q_1 \dots q_n]^T$. The terms 'joint coordinates' or 'internal coordinates' are commonly used for this vector in robotics.

This set of coordinates describes completely the relative motion of the links (Figure 2). With the basic link in the chain fixed, the system would have n DOFs. However, the basic link in the chain is not fixed but allowed to perform six independent motions in space. Let the position of the basic link be defined by the three Cartesian coordinates (x, y, z) of its mass center and the three orientation angles

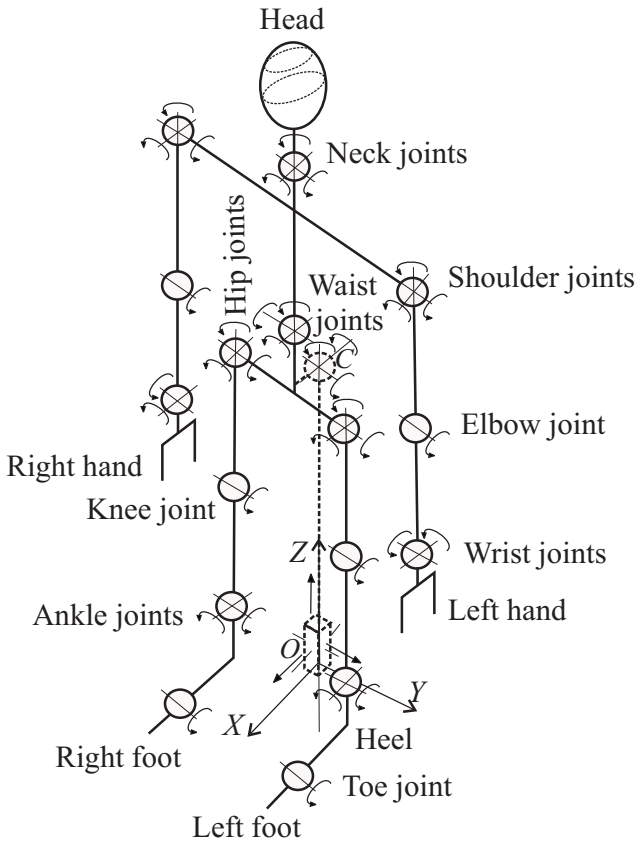

FIGURE 2. Kinematic scheme of a biped locomotion system used in simulation

(φ-roll, θ-pitch and ψ-yaw), forming the vector $\underline{X} = [x\ y\ z\ \varphi\ \theta\ \psi]^T$. Now, the overall number of DOFs for the system is $N = 6 + n$, and the system position is defined by

$$Q = [\underline{X}\ q]^T = [x\ y\ z\ \varphi\ \theta\ \psi\ q_1 \dots q_n]^T \tag{1}$$

It is assumed that each joint has an appropriate actuator. This means that each motion q_j has its own drive - the torque τ_j. Note that there is no drive associated to the basic body coordinates $\underline{X}$. The vector of the joint drives is $\tau = [\tau_1 \dots \tau_2]^T$, and the augmented drive vector (N-dimensional) is $T = [\underline{O}_6\ \tau]^T = [0 \dots 0\ \tau_1 \dots \tau_n]^T$. Similarly, with human beings muscles represent biological power-trains. Pairs of muscles by their synchronized contractions and extensions move the bones of the skeleton at its joints. The dynamic model of the biped mechanism (humanoid) has the general form [1, 7]:

$$\begin{aligned} &H(Q,d)\ddot{Q} + h(Q,\dot{Q},d) = \tau\ +\ J^T(Q,d)\,F \\ &h(Q,\dot{Q},d) = h_{ccf}(Q,\dot{Q},d) + h_g(Q,d) \end{aligned} \tag{2}$$

Dimensions of the inertial matrix is $H(N \times N)$. Dimensions of the vectors containing centrifugal, Coriolis' and gravity effects is $h(N \times 1)$. Vector $h(Q,d)$ consists of two vectors: $h_{ccf}(Q,\dot{Q},d)$ the vector of centrifugal and Coriolis' forces and the vector of gravity forces and moments $h_g(Q,d)$. Dimension of the vector of ground reaction,

external load and disturbance forces is: $F(m \times 1)$. Dimensions of the Jacobi matrix is $J(m \times N)$. Vector $d(l \times 1)$ represents a parameter vector including geometry (links' lengths, positions of the links' mass centers), as well as the corresponding dynamic parameters (links' masses, moments of inertia) of the robotic system. $J^T(Q, d)\, F$ describes the impact/contact term.

From the mechanical point of view, the stability of a humanoid robot is the most important criteria that try to reach by roboticians using mostly the Zero Moment Point (ZMP) theory [7]. This theory specifies the point with respect to which dynamic reaction force at the contact of the foot with the ground does not produce any moment (Figure 3).

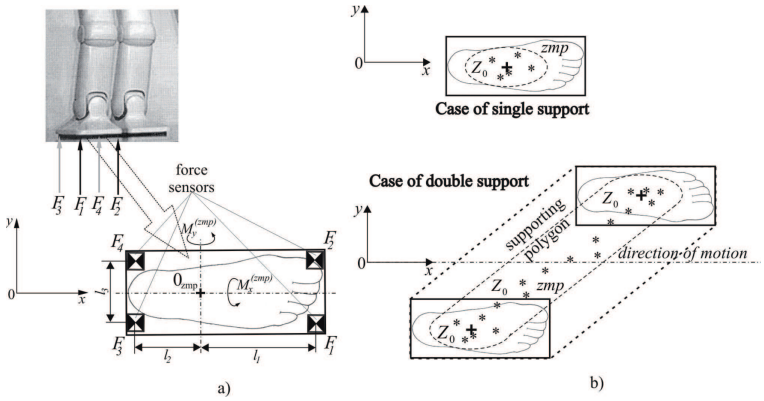

FIGURE 3. Zero-Moment Point illustration: a) Legs of a humanoid robot General arrangement of force sensors in determining the ZMP position; b) Zone of possible ZMP positions when the robot is in the state of dynamic balance

In the following sections we present two different frictional impact modelling starting with the Linear Complementarity Problem (LCP) then the impedance model.

3. **Modeling of foot contact dynamics via a LCP formulation.** Biped locomotion mechanisms are, due to the frictional impact/contact, called unilaterally constrained dynamical systems. Generally speaking, the normal contact expresses that the points in contact do not penetrate the ground and that the reaction force is always unidirectional. On the other hand linearized 3D Coulomb friction law, as shown in Figure 4, is considered.

In this section we follow the lines of [6] Let us consider the foot that moves towards the ground, strikes it and stays in contact. To express mathematically the forthcoming contact, the motion of the considered link should be described by an appropriate set of coordinates. Since the link is a body moving in the three dimensional space, it is necessary to consider six coordinates. Let this set be $\underline{g} = [g_1 \dots g_6]^T$ and let call them functional coordinates (Figure 5a). Functional coordinates are introduced [1] as relative ones, defining the position of the link with respect to the ground to be contacted.

A consequence of the rigid link-object contact is that the link and the object perform some motions, along some axes, jointly (Figure 5b). These are constrained

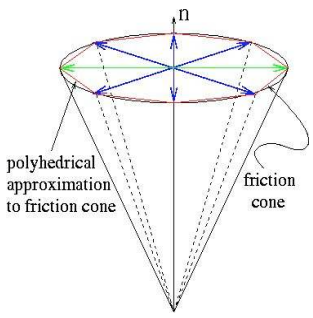

FIGURE 4. 3D Coulomb friction cone

(restricted) directions (e.g. g_3, g_5, Figure 5b). Let there be m such directions. Relative position along these axes does not change. Along the other axes (e.g. g_1, g_2, g_4, g_6, Figure 5b), relative displacement is possible. These are unconstrained (free) directions. In order to get a simple mathematical description of the contact, $\underline{g}$-coordinates are introduced to describe the relative position. Zero value of a coordinate indicates the contact along the corresponding axis.

So, the motion of the external object (to be contacted) has to be known (or calculated from the appropriate mathematical model), and then the $\underline{g}$-frame fixed to the object (the plane π in this case, Figure 5) is introduce to describe the relative position of the link in the most proper way. Thus, in a general case, the $\underline{g}$-frame is mobile. As the link is approaching the object, some of $\underline{g}$-coordinates reduce and finally reach zero. The zero value means that the contact is established. These functional coordinates (which reduce to zero) are called restricted coordinates and they form the subvector $\underline{g}^c$ of dimension m. The other functional coordinates are free and they form the subvector $\underline{g}^f$ of dimension $6-m$. Now, one can write:

$$[\underline{g}^c, \underline{g}^f] = K \cdot \underline{g} \tag{3}$$

where K is a 6×6 matrix used to rearrange the functional coordinates (elements of the vector $\underline{g}$) and bring the restricted ones to the first positions. In order to arrive at a general algorithm, the foot motion has to be described in a general way and, once the expected contact is specified, relate this general interpretation to the appropriate $\underline{s}$-frame.

The general description of the link motion assumes three Cartesian coordinates of a selected point of the link plus three orientation angles: $\underline{s}_l = [x_l\ y_l\ z_l\ \varphi_l\ \theta_l\ \psi_l]^T$, the subscript l standing for "link". These are absolute external coordinates in the $Oxyz$ reference coordinate system (Figure 5a). The relation between the link coordinates $\underline{s}_l$ and the system position vector Q defined in (1) is given by:

$$\underline{s}_l = \underline{s}_l(Q, d) \tag{4}$$

$$\dot{\underline{s}}_l = J_l(Q, d)\dot{Q} \tag{5}$$

$$\ddot{\underline{s}}_l = J_l(Q, d)\ddot{Q} + A_l(Q, \dot{Q}, d) \tag{6}$$

where $J_l = \frac{\partial \underline{s}_l}{\partial Q}$ is a $6 \times N$ Jacobian matrix and $A_l = \frac{\partial^2 \underline{s}_l}{\partial Q^2}\dot{Q}^2$ is a 6-dimensional adjoint vector. Let us concentrate on the object, i.e. the ground (example of an immobile object). In a general case, the object is mobile, so, its position is described

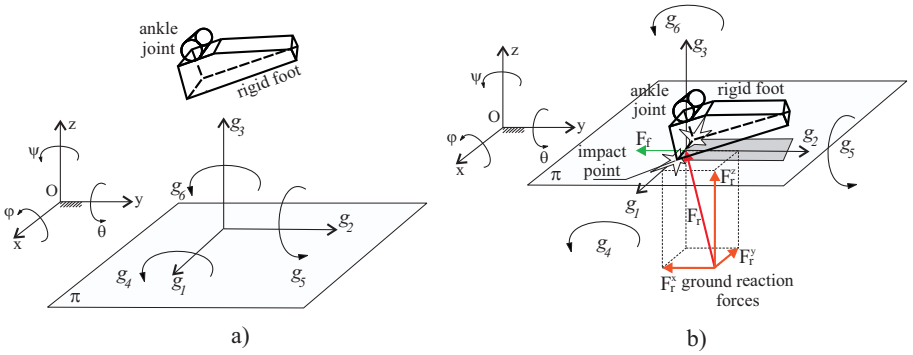

FIGURE 5. a) Functional coordinates of the foot contact; b) Rigid frictional impact along the foot edge

by the absolute external coordinates: $\underline{s_b} = [x_b \ y_b \ z_b \ \varphi_b \ \theta_b \ \psi_b]^T$, the subscript b standing for "object".

When the $\underline{g}$-frame is introduced to define the relative position of the link with respect to the object, the coordinates will depend on both $\underline{s_l}$ and $\underline{s_b}$:

$$\underline{g} = \underline{g}(\underline{s_l}, \underline{s_b}) \tag{7}$$

or in the Jacobian form:

$$\dot{\underline{g}} = J_{gl}\dot{\underline{s}}_l + J_{gb}\dot{\underline{s}}_b \tag{8}$$

$$\ddot{\underline{g}} = J_{gl}\ddot{\underline{s}}_l + J_{gb}\ddot{\underline{s}}_b + A_g. \tag{9}$$

where the dimension of the Jacobi matrices is $J_{gl}, J_{gb} \in \mathbb{R}^{6\times 6}$, and the dimension of the adjoint vector $A_g \in \mathbb{R}^{6\times 6}$. Model (9) can be rewritten if the separation (3) is introduced. The model becomes:

$$\ddot{\underline{g}}^c = J^c_{gl}\ddot{\underline{s}}_l + J^c_{gb}\ddot{\underline{s}}_b + A^c_g. \tag{10}$$

$$\ddot{\underline{g}}^f = J^f_{gl}\ddot{\underline{s}}_l + J^f_{gb}\ddot{\underline{s}}_b + A^f_g. \tag{11}$$

The object motion, $\underline{s_b}(t)$ in equations (7)-(9), is either prescribed or calculated from a separate mathematical model of the object. Equations (10) and (11) can be rewritten if (6) is introduced:

$$\ddot{\underline{g}}^c = J^c_{gl}J_l\ddot{Q} + J^c_{gl}A_l + J^c_{gb}\ddot{\underline{s}}_b + A^c_g = J^c_{g,TOT}(Q,t)\ddot{Q} + A^c_{g,TOT}(Q,\dot{Q},t). \tag{12}$$

$$\ddot{\underline{g}}^f = J^f_{gl}J_l\ddot{Q} + J^f_{gl}A_l + J^f_{gb}\ddot{\underline{s}}_b + A^f_g = J^f_{g,TOT}(Q,t)\ddot{Q} + A^f_{g,TOT}(Q,\dot{Q},t). \tag{13}$$

where the model matrices are: $J^c_{g,TOT} = J^c_{gl}J_l$, $A^c_{g,TOT} = J^c_{gl}A_l + J^c_{gb}\ddot{\underline{s}}_b + A^c_g$, $J^f_{g,TOT} = J^f_{gl}J_l$ and $A^f_{g,TOT} = J^f_{gl}A_l + J^f_{gb}\ddot{\underline{s}}_b + A^f_g$.

In this paper we consider the case which encompasses rigid, durable lasting contacts. This means that the two bodies (the biped and the object), when the impact of touching each other is over, continue to move together for some finite time. The example is walking. When the foot touches the ground, it will keep the contact for some time before it moves up again. It is clear that a general theory of impact, including the elasto-dynamic effects, can cover all the mentioned contacts. So, we are going to elaborate in detail one representative type of contact - rigid, durable contact.

3.1. **Modeling of a rigid, durable contact with object - three phases.** This section elaborates:

- rigid contact - allowing no deformation between the two bodies;
- the case of the object motion that is given and cannot be influenced by the biped (thus, $\underline{s}_b(t)$ is considered as given);
- durable contact lasting for a finite time after the impact.

One may recognize the three phases of such contact task [1, 7]: (i) approaching, (ii) impact, and (iii) regular contact motion.

The first phase is approaching. The link moves towards the object. All functional coordinates $\underline{g}$ are free but some of them (the subvector $\underline{g}^c$) reduce to zero.

The second phase is the impact. In the preceding phase (approaching), the motion of the link was planned so as to reach the object with a relative velocity equal to zero (collision-free contact). This is the reference motion. However, the control system produces the actual motion different from the reference. The tracking error leads to collision, a non-zero-velocity contact. The impact forces will affect the system state - after the impact the link state will comply with the object state and the type of contact.

The third phase is the regular contact motion. The contact forces make the link move according to the character of the contact.

We now elaborate these phases starting with the first one. The third phase (regular contact motion) will be discussed before the second phase (impact) since it is more convenient for the mathematical method applied.

First phase of contact task - approaching. The approaching step is an unconstrained (free) motion. Although all coordinates from the vector $\underline{g}$ are free, we use the separation (3) since the subvector $\underline{g}^c$ is intended to describe the coming contact.

Dynamics of the approaching is described by the model (2). The model represents the set of N scalar equations that can be solved for N scalar unknowns - the acceleration vector $\ddot{Q}$ (thus enabling integration and calculation of the system motion $Q(t)$). The link motion in the absolute external frame, $\underline{s}_l$, is calculated by using (6). For the approaching phase, it is more interesting to observe functional coordinates. Since the object motion $\underline{s}_b$ is given, relation (9) (or (10), (11)) allows one to calculate the link functional trajectory $\underline{g}(t)$.

The reference motion $\underline{g}_0(t)$ is planned so as to make a zero-velocity contact at the instant $t_c^0 : \underline{g}_0(t_c^0) = \underline{0} :$ and $\dot{\underline{g}}_0(t_c^0) = \underline{0}$. Due to the control system, tracking error will appear and the actual motion will differ from the reference. So, it is necessary to monitor the coordinates $\underline{g}^c$ and detect the contact as the instant t_c' when $\underline{g}^c$ reduces to zero ($\underline{g}(t_c') = \underline{0}$). It will be $t_c' \neq t_c^0$, and the contact velocity will not be zero: $\dot{\underline{g}}(t_c') \neq \underline{0}$.

During the approaching, the integration of the system coordinates Q is done. So, at the instant of impact, there will be some system state $Q(t_c'), \dot{Q}(t_c')$.

Third phase of contact task - regular contact motion. Regular contact motion starts when the transient effects of the impact vanish. In this phase the restricted coordinates are kept zero. So,

$$\underline{g}^c(t) = \underline{0} \tag{14}$$

and accordingly

$$\dot{\underline{g}}^c(t) = \underline{0}, \quad \ddot{\underline{g}}^c(t) = \underline{0}. \tag{15}$$

Now, relation (12) is replaced with

$$J^c_{g,TOT}(Q,t)\,\ddot{Q} + A^c_{g,TOT}(Q,\dot{Q},t) = \underline{0} \tag{16}$$

while relation (13) still holds:

$$\ddot{\underline{g}}^f = J^f_{g,TOT}(Q,t)\,\ddot{Q} + A^f_{g,TOT}(Q,\dot{Q},t).$$

In contact problems, the dynamic model has to take care of contact forces. Model (2), derived for a free biped, should be supplemented by contact forces. A contact force acts along each of constrained axis. So, there is a reaction force (or torque) for each coordinate from the set $\underline{g}^c$. There are m independent reactions. Let $F_r = [F_1, \cdots, F_m]^T$ be the reaction vector. If a coordinate g^c_j is linear (translational), then the corresponding reaction F_j is a force. For a revolute coordinate, the corresponding reaction is a torque.

The contact-dynamics model is obtained by introducing reactions into the biped model (2):

$$H(Q,d)\ddot{Q} + h(Q,\dot{Q},d) = \tau + J^c_{g,TOT}(Q,d,t)^T F_r \tag{17}$$

Since this model involves N scalar equations and $N+m$ scalar unknowns (vectors $\ddot{Q}$ and F_r), it is necessary to supply some additional conditions. The additional condition is the constraint relation (16), containing m scalar equations. So, (17) and (16) describe the dynamics of a constrained biped, allowing one to calculate the acceleration $\ddot{Q}$ and reaction F_r (thus enabling the integration and calculation of the system motion).

Second phase of contact task - impact. The impact phase starts when the biped link reaches the surrounding object(s). Strictly speaking, the restricted coordinates (elements of $\underline{g}^c$) reach zero one by one. So, a complex contact is established as a series of simpler contact effects. According to [1] the impact model is derived assuming that all the coordinates $\underline{g}^c$ attain zero simultaneously and establish a complex contact instantaneously. Let t'_c be the instant when the contact is established (restricted coordinates reduce to zero and the impact comes into action) and let t''_c be the instant when the impact ends. So, the impact lasts for $\Delta t = t''_c - t'_c$. For this analysis we assume that the impact is infinitely short, i.e. $\Delta t \to 0$. We also assume that the m coordinates (forming $\underline{g}^c$) reduce to zero simultaneously. We now integrate the dynamic model (17) over the short impact interval Δt:

$$H\,\Delta\dot{Q} = (J^c_{g,TOT})^T\,F_r\,\Delta t \tag{18}$$

where

$$\Delta\dot{Q} = \dot{Q}(t''_c) - \dot{Q}(t'_c) = \dot{Q}'' - \dot{Q}'. \tag{19}$$

During the approaching phase, the system model is integrated and the motion $Q(t), \dot{Q}(t)$ is calculated. Thus, the state at the instant t'_c, i.e. $Q' = Q(t'_c)$, $\dot{Q}' = \dot{Q}(t'_c)$, is considered known. Since the object motion is also known, it is possible to calculate the model matrices H , $J^c_{g,TOT}$ in equation (18). The position does not change during $\Delta t \to 0$, and hence: $Q'' = Q(t''_c) = Q'$. Now, the model (18) (along with (19)), contains N scalar equations with $N+m$ scalar unknowns: the velocity after the impact, $\dot{Q}'' = \dot{Q}(t''_c)$ (dimension N), and the impact momentum $F_r\Delta t$ (dimension m). The additional equations needed to allow solution are obtained starting from the constraint relation (16). Integrating (16) over $\Delta t \to 0$, one obtains

$$J^c_{g,TOT}(Q,t)\,\Delta\,\dot{Q} = 0 \tag{20}$$

i.e. the additional m scalar conditions. The augmented set of equations (18) and (20) (along with (19)) allow to solve the impact. The velocity after the impact, $\dot{Q}'' = \dot{Q}(t_c'')$, is found starting from the known state in t_c'. The impact momentum $F_r \Delta t$ is determined as well. The new state Q'', $\dot{Q}''$ represents the initial condition for the third phase, i.e. the regular contact motion (explained in the previous paragraph).

Another approach, which is more realistic than an idealized single-point contact considered previously, deals with multi-point frictional contact of the biped's feet. In this case, the restricted coordinates (elements of $\underline{g}^c$) reach zero one by one. The impact begins when the biped foot (feet) reaches the constraint surface π as presented in Figure 3.1. Constraint in a general case can be an ordinary curve, prismatic or flat surface. In the impact phase, the restricted coordinates $\underline{g}^c$ defined in (3) become zero. The existence of impact can be defined by the following conditions:

$$\underline{g}^c(t) = \underline{0}, \ \dot{\underline{g}}^c(t) \leq \underline{0}. \tag{21}$$

In a general case, a foot impact to the constraint surface can be realized at an infinite number of points. Consequently, the problem would be numerically too complex. Because of that, a realistic approximation of the impact phenomenon has to be assumed. Without losing generality, four impact points (per foot contour $i = 1, \ldots, 4$ or $i = 5, \ldots, 8$, see Figure 3.1) instead of an infinite number of them can be assumed. Here, two contact points at the heel (i.e. $i = 1, 2$ and $i = 5, 6$, Figure 3.1) and two points at the front part of the foot (i.e. $i = 3, 4$ and $i = 7, 8$) will be considered. Generally, three possible unilateral impacts are possible: (i) single-point impact, (ii) two-points impact along the ordinary foot edge (e.g. the points $i = 5, 6$, Figure 3.1), and (iii) four-points impact (the case of a planar impact of the flat foot sole to the support). By considering the impact phenomenon as a series of simpler, unilateral contacts at the particular points one can perform a realistic analysis of the non-smooth, frictional biped contact dynamics.

Having in mind the above, some general assumptions should be put forward before deriving the non-smooth, multi-point impact model:

- The duration of the impact is "very short" $\Delta t(i) \to 0$.
- Bodies' impact can be generally divided in two phases: the compression phase and the expansion phase. Since the foot impact is followed by the compression phase, after which the biped foot stays completely or partly lying (pressed by biped weight) on the constraint surface, the expansion phase appears only in the special cases and will not be considered. The end of the compression phase is the start of the regular contact.
- While the impact takes place (in the time interval Δt) the values of all the quantities of the multi-body system (biped mechanism) characterizing its position and orientation, as well as all non-impulse forces and torques (gravity, centrifugal and Coriolis'), remain constant.
- Wave effects (elastic modes in the system) are not taken into account.

In the multiple-contact tasks such as biped gait, for example, there may occur only one impact at one of the potential contact points or several impacts at several contacts simultaneously. The theory presented in the paper covers both possibilities. Here we will consider a system with $N_G = 8$ possible contact points. For this purpose four sets of indices are introduce to describe the kinematic state of each of the contacts. Let then:

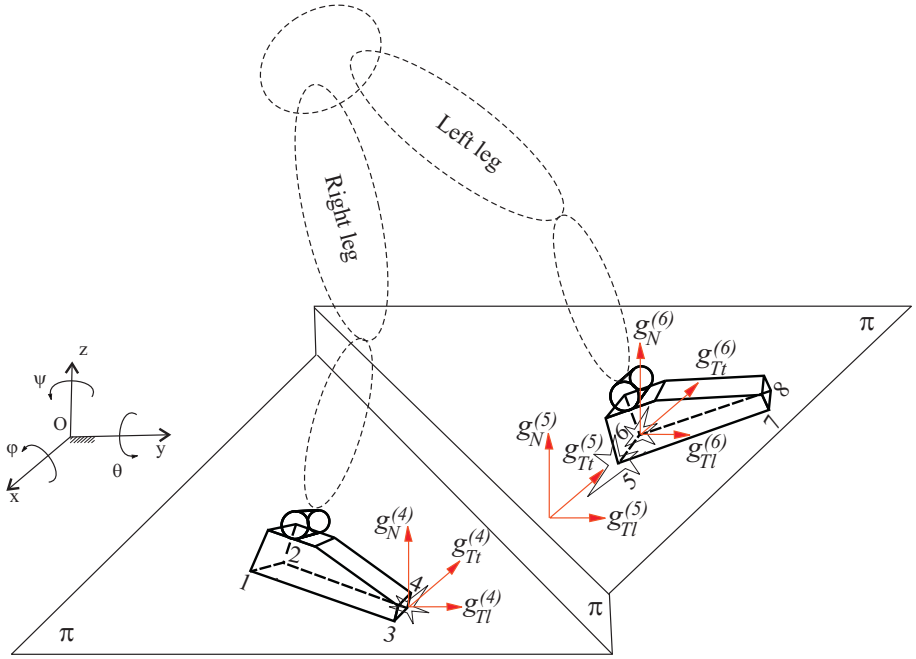

FIGURE 6. Multi-point contacts of the biped links with the constraint surface π - the normal g_N^i and the tangential directions $g_{Tl}^{(i)}$, $g_{Tt}^{(i)}$ of motion of the particular points $i = 1, \ldots, 8$.

$$
\begin{aligned}
&\Omega_G = \{1, 2, \ldots, n_G\}, \Omega_S = \left\{ i \in \Omega_G \mid g_N^{(i)} = 0 \right\} \text{ with } n_S \text{ elements} \\
&\Omega_N = \left\{ i \in \Omega_S \mid \dot{g}_N^{(i)} = 0 \right\} \text{ with } n_N \text{ elements,} \\
&\Omega_{H1} = \left\{ i \in \Omega_N \mid \dot{g}_{Tl}^{(i)} = 0 \right\} \text{ with } n_{H1} \text{ elements,} \\
&\Omega_{H2} = \left\{ i \in \Omega_N \mid \dot{g}_{Tt}^{(i)} = 0 \right\} \text{ with } n_{H2} \text{ elements.}
\end{aligned} \tag{22}
$$

The locations of the impacts are given by the positions of the n_G contact points of Ω_G. Ω_S contains n_S indices of the constraints with vanishing distance but arbitrary relative velocities, Ω_N describes the constraints which fulfil the necessary conditions for continuous contact (vanishing distance and zero relative velocity in the normal direction), and Ω_{H1}, Ω_{H2} are those which are possibly sticking in two tangential directions - longitudinal and transversal. Numbers of elements of the sets Ω_S, Ω_N, Ω_{H1}, Ω_{H2} are not constant because the contact configuration of the biped mechanism changes with time due to the stick-slip transitions, impacts and contact loss.

For each contact point from Ω_G it is possible to determine the distance $g_N^{(i)}(Q,t)$ along the normal direction to the constraint surface. If one of these indicators becomes zero at the time instant $t_c'(i)$ and the corresponding relative velocity $\dot{g}_N^{(i)}$ is smaller than or equal to zero, an impact occurs. The contact is then closed and the unilateral constraint is active. The set od constraints which participate in the impact is then given by

$$
\Omega_S^* = \left\{ i \in \Omega_G \mid g_N^{(i)} = 0;\ \dot{g}_N^{(i)} \leq 0 \right\} \quad \text{with } n_S^* \text{ elements.} \tag{23}
$$

The set Ω_S^* contains all the sliding and sticking continuous-contact constraints ($g_N^{(i)} = 0$), as well as the impact contacts ($\dot{g}_N^{(i)} \leq 0$). This enables one to examine whether a contact separates under the influence of an impact at a different location i.

In order to determine the multi-point impact model, let us introduce the following functional coordinates $\underline{g}^{(i)}$, $i \in \Omega_S^*$ (see Figure 3.1). Instead of using the unified $\underline{g}(6 \times 1)$-vector of the functional coordinates (defined by (3)), the set of $n_S^*(3 \times 1)$-vectors of the functional coordinates $\underline{g}^{(i)}$, $i \in \Omega_S^*$ will be introduced. In such a way, the relative positions of the biped feet are determined in the $\underline{g}^{(i)}$-frames, as shown in Figure 3.1. Functional coordinates $\underline{g}^{(i)}$ represent relative positions of the feet points i with respect to the corresponding frame attached to the constraint surface. In that sense, the normal $g_N^{(i)}$ and the tangential directions $g_{Tl}^{(i)}$ and $g_{Tt}^{(i)}$ are important. Tangential motions of the feet points are possible along the longitudinal $g_{Tl}^{(i)}$ as well along the transversal $g_{Tt}^{(i)}$ coordinate axes (Figure 3.1). The i-th vector of the functional coordinates $\underline{g}^{(i)}$, $i \in \Omega_S^*$ can be written in the form:

$$\underline{g}^{(i)} = \left[g_{Tl}^{(i)},\ g_{Tt}^{(i)},\ g_N^{(i)} \right]^T,\ i \in \Omega_S^*. \tag{24}$$

Bearing in mind the vector form (24), three components of impact forces can be defined in the same directions. They are: the normal impact force F_{N_i} in the $g_N^{(i)}$-direction of the restricted motion and the tangential impact forces F_{Tl_i}, F_{Tt_i} in the longitudinal $g_{Tl}^{(i)}$- and transversal $g_{Tt}^{(i)}$-directions. In a physical sense, the considered tangential forces represent the corresponding stick/slip frictional forces acting in the plane that represents a constraint. The (3×1) vector F_{C_i} of the impact force acts at the i-th contact point C_i , $i \in \Omega_S^*$, and can be defined in the form:

$$F_{C_i} = [F_{Tl_i},\ F_{Tt_i},\ F_{N_i}]^T, i \in \Omega_S^*. \tag{25}$$

Positions of the contact points C_i, $i \in \Omega_S^*$ are always in the constraint area (or belong to the object that represents a constraint), and they are determined in the inertial coordinate system $Oxyz$. Let now $t_c'(i)$ be the instant when the i-th contact point of the foot and the constraint is established (i.e. when the restricted coordinate in the normal direction $g_N^{(i)}$ reduce to zero $g_N^{(i)} = 0$ and the impact comes into action $\|F_{C_i}\| > 0$) and let $t_c''(i)$ be the instant when the impact of the i-th point ends. So, the impact lasts for the time period $\Delta t(i) = t_c''(i) - t_c'(i)$.

When the $\underline{g}^{(i)}$-frame (defined by (24)) is introduced to determine the relative position of the i-th contour point at the foot with respect to the position of the contact C_i (lying in the constraint plane π, Figure 3.1), the coordinates $\underline{g}^{(i)}$ depend on both external coordinates $\underline{s}_{C_i}$ and $\underline{s}_{\pi_i}$:

$$\underline{g}^{(i)} = \underline{g}^{(i)}(\underline{s}_{C_i}, \underline{s}_{\pi_i}), \quad i \in \Omega_S^*. \tag{26}$$

$\underline{s}_{C_i}(Q,t) = \left[s_{C_i}^x,\ s_{C_i}^y,\ s_{C_i}^z \right]^T$ and $\underline{s}_{\pi_i}(t) = \left[s_{\pi_i}^x,\ s_{\pi_i}^y,\ s_{\pi_i}^z \right]^T$ are (3×1)-vectors that define position of the contact C_i of the biped foot as well as position of the corresponding point of the constraint surface π to be reached during the impact. The positions $\underline{s}_{C_i}$ and $\underline{s}_{\pi_i}$ are determined with respect to the inertial coordinate system $Oxyz$ (Figure 3.1). Then, a Jacobian form can be written as:

$$\dot{\underline{g}}^{(i)} = \left[\dot{g}_{Tl}^{(i)},\ \dot{g}_{Tt}^{(i)},\ \dot{g}_N^{(i)} \right]^T = J_{gC_i} \dot{\underline{s}}_{Ci} + J_{g\pi_i} \dot{\underline{s}}_{\pi_i}, \quad i \in \Omega_S^* \tag{27}$$

Equation (27) can be projected onto the $\underline{g}^{(i)}$-frame axes $g_N^{(i)},\ g_{Tl}^{(i)},\ g_{Tt}^{(i)}$, (Figure 3.1). For this purpose three 3×1 unit vectors $\tilde{n}_i,\ \tilde{t}_{l_i},\ \tilde{t}_{t_i}$ (collinear with the corresponding axes $g_N^{(i)},\ g_{Tl}^{(i)},\ g_{Tt}^{(i)}$, of the i-th system) are introduced. Then, equation (27) can be re-written in a scalar form:

$$\begin{array}{l}\dot{g}_N^{(i)} = \tilde{n}_i^T J_{gC_i}\,\underline{\dot{s}}_{C_i} + \tilde{n}_i^T J_{g\pi_i}\underline{\dot{s}}_{\pi_i},\\ \dot{g}_{Tl}^{(i)} = \tilde{t}_{l_i}^T J_{gC_i}\,\underline{\dot{s}}_{C_i} + \tilde{t}_{l_i}^T J_{g\pi_i}\underline{\dot{s}}_{\pi_i},\quad i\in\Omega_S^*\\ \dot{g}_{Tt}^{(i)} = \tilde{t}_{t_i}^T J_{gC_i}\,\underline{\dot{s}}_{C_i} + \tilde{t}_{t_i}^T J_{g\pi_i}\underline{\dot{s}}_{\pi_i}.\end{array} \tag{28}$$

where $J_{gC_i},\ J_{g\pi_i}$are 3×3 Jacobian matrices defined in (27). The motion of the constraint surface $\underline{\dot{s}}_{\pi_i}$ (in the case when it is mobile) is either prescribed or calculated from a separate mathematical model of the object (constraint). If the following kinematic relations are introduced:

$$\underline{s}_{C_i} = \underline{s}_{C_i}(Q,t),\quad i\in\Omega_S^*. \tag{29}$$

$$\underline{\dot{s}}_{C_i} = J_{C_i}(Q)\,\dot{Q},\quad i\in\Omega_S^*. \tag{30}$$

then equations (28) can be expanded to acquire the form:

$$\begin{array}{l}\dot{g}_N^{(i)} = \tilde{n}_i^T J_{gC_i}J_{C_i}(Q)\cdot\dot{Q} + \tilde{n}_i^T J_{g\pi_i}\underline{\dot{s}}_{\pi_i} = J_{gC_i,TOT}^N\,\dot{Q} + A_{g\pi_i}^N,\\ \dot{g}_{Tl}^{(i)} = \tilde{t}_{l_i}^T J_{gC_i}J_{C_i}(Q)\cdot\dot{Q} + \tilde{t}_{l_i}^T J_{g\pi_i}\underline{\dot{s}}_{\pi_i} = J_{gC_i,TOT}^{Tl}\,\dot{Q} + A_{g\pi_i}^{Tl},\quad i\in\Omega_S^*\\ \dot{g}_{Tt}^{(i)} = \tilde{t}_{t_i}^T J_{gC_i}J_{C_i}(Q)\cdot\dot{Q} + \tilde{t}_{t_i}^T J_{g\pi_i}\underline{\dot{s}}_{\pi_i} = J_{gC_i,TOT}^{Tt}\,\dot{Q} + A_{g\pi_i}^{Tt}\end{array} \tag{31}$$

where $J_{C_i} = \frac{\partial \underline{s}_{C_i}(Q)}{\partial Q}$ is a $(3\times N)$ Jacobian matrix defining the dependence of the linear velocity $\underline{\dot{s}}_{C_i}$ of the i-th point as a function of the generalized coordinates $\dot{Q}$; $J_{gC_i,TOT}^N = \tilde{n}_i^T J_{gC_i}J_{C_i}(Q),\quad J_{gC_i,TOT}^{Tl} = \tilde{t}_{l_i}^T J_{gC_i}J_{C_i}(Q)$, and $J_{gC_i,TOT}^{Tt} = \tilde{t}_{t_i}^T J_{gC_i}J_{C_i}(Q)$ are the $(1\times N)$ total Jacobian matrices; $A_{g\pi_i}^N = \tilde{n}_i^T J_{g\pi_i}\underline{\dot{s}}_{\pi_i},\quad A_{g\pi_i}^{Tl} = \tilde{t}_{l_i}^T J_{g\pi_i}\underline{\dot{s}}_{\pi_i}$, and $A_{g\pi_i}^{Tt} = \tilde{t}_{t_i}^T J_{g\pi_i}\underline{\dot{s}}_{\pi_i}$ are the corresponding adjoint scalars from (31).

Taking into account the previous consideration, as well as the contact force vector (25), the contact-dynamics model (17) can be rewritten in the form that includes multi-point contact effects:

$$H(Q)\,\ddot{Q}+h(Q,\dot{Q}) = \tau+\sum_{i\in\Omega_S^*} J_{gC_i,TOT}^{N^T}\cdot F_{N_i}+\sum_{i\in\Omega_S^*} J_{gC_i,TOT}^{Tl^T}\cdot F_{Tl_i}+\sum_{i\in\Omega_S^*} J_{gC_i,TOT}^{Tt^T}\cdot F_{Tt_i}. \tag{32}$$

After certain rearrangement and simplification of the designation the relation (32) can be written in a form that is suitable for deriving impact equations:

$$H\,\ddot{Q}+\tilde{h}-\sum_{i\in\Omega_S^*} J_{gC_i,TOT}^{N^T}\cdot F_{N_i}-\sum_{i\in\Omega_S^*} J_{gC_i,TOT}^{Tl^T}\cdot F_{Tl_i}-\sum_{i\in\Omega_S^*} J_{gC_i,TOT}^{Tt^T}\cdot F_{Tt_i} = \underline{0}. \tag{33}$$

where $\tilde{h} = h-\tau$ is an $(N\times1)$ vector taking into account the gravity and centrifugal effects, as well as the driving torques at the biped's joints. Kinematic and dynamic relations (31) and (33) represent the basis for the development of the impact model of biped gait. Let us write them in a matrix notation:

$$\begin{bmatrix}\underline{\dot{g}}_N\\ \underline{\dot{g}}_{Tl}\\ \underline{\dot{g}}_{Tt}\end{bmatrix} = \begin{bmatrix}W_N\\ W_{Tl}\\ W_{Tt}\end{bmatrix}\dot{Q}+\begin{bmatrix}\tilde{\omega}_N\\ \tilde{\omega}_{Tl}\\ \tilde{\omega}_{Tt}\end{bmatrix}. \tag{34}$$

$$H\,\ddot{Q}+\tilde{h}-\begin{bmatrix}W_N^T & W_{Tl}^T & W_{Tt}^T\end{bmatrix}\cdot\begin{bmatrix}F_N\\ F_{Tl}\\ F_{Tt}\end{bmatrix} = \underline{0}. \tag{35}$$

where: $\underline{\dot{g}}_N = \left[\dot{g}_N^{(1)} \dots \dot{g}_N^{(n_S^*)}\right]^T$, $\underline{\dot{g}}_{Tl} = \left[\dot{g}_{Tl}^{(1)} \dots \dot{g}_{Tl}^{(n_S^*)}\right]^T$, $\underline{\dot{g}}_{Tt} = \left[\dot{g}_{Tt}^{(1)} \dots \dot{g}_{Tt}^{(n_S^*)}\right]^T$ are $(n_S^* \times 1)$ integrated vectors of the relative body (foot) velocities in the normal and tangential coordinate directions of motion; $W_N = \left[J^N_{gC_1,TOT} \dots J^N_{gC_{n_S^*},TOT}\right]^T$, $W_{Tl} = \left[J^{Tl}_{gC_1,TOT} \dots J^{Tl}_{gC_{n_S^*},TOT}\right]^T$ and $W_{Tt} = \left[J^{Tt}_{gC_1,TOT} \dots J^{Tt}_{gC_{n_S^*},TOT}\right]^T$ are Jacobian matrices determined for the motions in the normal and tangential directions; $\tilde{\omega}_N = \left[A^N_{g\pi_1} \dots A^N_{g\pi_{n_S^*}}\right]^T$, $\tilde{\omega}_{Tl} = \left[A^{Tl}_{g\pi_1} \dots A^{Tl}_{g\pi_{n_S^*}}\right]^T$, $\tilde{\omega}_{Tt} = \left[A^{Tt}_{g\pi_1} \dots A^{Tt}_{g\pi_{n_S^*}}\right]^T$ are $(n_S^* \times 1)$ vectors of the adjoint scalars defined in the kinematic relations (34); $F_N = \left[F_{N_1} \dots F_{N_{n_S^*}}\right]^T$, $F_{Tt} = \left[F_{Tl_1} \dots F_{Tl_{n_S^*}}\right]^T$, $F_{Tt} = \left[F_{Tt_1} \dots F_{Tt_{n_S^*}}\right]^T$ are $(n_S^* \times 1)$ vectors of normal and tangential impact forces.

After integrating equation (35) over the impact period $\Delta t_{c_i} = t''_{c_i} - t'_{c_i}$, $i \in \Omega_S^*$, the following expression is derived:

$$H\left(\dot{Q}'' - \dot{Q}'\right) - \left[W_N^T \quad W_{Tl}^T \quad W_{Tt}^T\right] \cdot \begin{bmatrix} \Lambda_N(t'_c) \\ \Lambda_{Tl}(t'_c) \\ \Lambda_{Tt}(t'_c) \end{bmatrix} = \underline{0}. \tag{36}$$

Here $\Lambda_N(t'_c)$, $\Lambda_{Tl}(t'_c)$, $\Lambda_{Tt}(t'_c)$ are the impulse momentums in the normal and tangential diretions which are transferred during the impact. They can be defined in the following way:

$$\begin{aligned} \Lambda_N &= \left[F_{N_1}\Delta t_{c_1}, \dots, F_{N_{n_S^*}}\Delta t_{c_{n_S^*}}\right]^T, \Lambda_{Tl} = \left[F_{Tl_1}\Delta t_{c_1}, \dots, F_{Tl_{n_S^*}}\Delta t_{c_{n_S^*}}\right]^T, \\ \Lambda_{Tt} &= \left[F_{Tt_1}\Delta t_{c_1}, \dots, F_{Tt_{n_S^*}}\Delta t_{c_{n_S^*}}\right]^T \end{aligned}$$

Knowing that $\dot{Q}' = \dot{Q}(t'_c)$ and $\dot{Q}'' = \dot{Q}(t''_c)$ are the instances of start and termination of the impact, the relative velocities at these instants can be defined:

$$\begin{bmatrix} \underline{\dot{g}}_N(t'_c) \\ \underline{\dot{g}}_{Tl}(t'_c) \\ \underline{\dot{g}}_{Tt}(t'_c) \end{bmatrix} = \begin{bmatrix} W_N \\ W_{Tl} \\ W_{Tt} \end{bmatrix} \dot{Q}' + \begin{bmatrix} \tilde{\omega}_N \\ \tilde{\omega}_{Tl} \\ \tilde{\omega}_{Tt} \end{bmatrix}; \begin{bmatrix} \underline{\dot{g}}_N(t''_c) \\ \underline{\dot{g}}_{Tl}(t''_c) \\ \underline{\dot{g}}_{Tt}(t''_c) \end{bmatrix} = \begin{bmatrix} W_N \\ W_{Tl} \\ W_{Tt} \end{bmatrix} \dot{Q}'' + \begin{bmatrix} \tilde{\omega}_N \\ \tilde{\omega}_{Tl} \\ \tilde{\omega}_{Tt} \end{bmatrix} \tag{37}$$

From the relations defined in (37), it is possible to derive the following functional dependence between the relative velocities in two characteristic instances t'_c and t''_c of the impact. Then:

$$\begin{bmatrix} \underline{\dot{g}}_N(t''_c) \\ \underline{\dot{g}}_{Tl}(t''_c) \\ \underline{\dot{g}}_{Tt}(t''_c) \end{bmatrix} = \begin{bmatrix} W_N \\ W_{Tl} \\ W_{Tt} \end{bmatrix} \left(\dot{Q}'' - \dot{Q}'\right) + \begin{bmatrix} \underline{\dot{g}}_N(t'_c) \\ \underline{\dot{g}}_{Tl}(t'_c) \\ \underline{\dot{g}}_{Tt}(t'_c) \end{bmatrix}. \tag{38}$$

Expressing the $\dot{Q}' - \dot{Q}''$ from (36) and including it in (38), the model of the unilateral multi-point impact of the biped locomotion system is derived:

$$\begin{bmatrix} \underline{\dot{g}}_N(t''_c) \\ \underline{\dot{g}}_{Tl}(t''_c) \\ \underline{\dot{g}}_{Tt}(t''_c) \end{bmatrix} = \begin{bmatrix} W_N \\ W_{Tl} \\ W_{Tt} \end{bmatrix} H^{-1} \left[W_N^T W_{Tl}^T W_{Tt}^T\right] \cdot \begin{bmatrix} \Lambda_N(t'_c) \\ \Lambda_{Tl}(t'_c) \\ \Lambda_{Tt}(t'_c) \end{bmatrix} + \begin{bmatrix} \underline{\dot{g}}_N(t'_c) \\ \underline{\dot{g}}_{Tl}(t'_c) \\ \underline{\dot{g}}_{Tt}(t'_c) \end{bmatrix}. \tag{39}$$

The model (39) consists of $3n_S^*$ scalar equations for $6n_S^*$ unknowns. Thus, $3n_S^*$ conditions must yet be formulated in order to determine the transferred impulses $\Lambda_N(t'_c)$, $\Lambda_{Tl}(t'_c)$, $\Lambda_{Tt}(t'_c)$ and the relative velocities $\underline{\dot{g}}_N(t''_c)$, $\underline{\dot{g}}_{Tl}(t''_c)$, $\underline{\dot{g}}_{Tt}(t''_c)$ at the end of the impact.

The normal impulse of compression results from integration of the normal force over the phase of compression:

$$\Lambda_{N_i} = \lim_{t'_{c_i} \to t''_{c_i}} \int_{t'_{C_i}}^{t''_{C_i}} F_{N_i}\, dt, \quad i \in \Omega_S^*. \tag{40}$$

where, because of the unilateral character of contact constraint, only compressive forces are possible:

$$F_{N_i}(t) \geq 0 \quad \forall \quad t \in [t'_{c_i}, t''_{c_i}]. \tag{41}$$

Thus, integrating (40) the normal forces with the property (41) results in non-negative values of the normal impulses:

$$\Lambda_{N_i} \geq 0, \quad i \in \Omega_S^*. \tag{42}$$

If the impulse (42) is transferred, then the corresponding contact participates in the impact and the end of compression is given by $\dot{g}_N^{(i)} = 0$. Thus, the allowed velicities correspond to $\dot{g}_N^{(i)} \geq 0$. The overall behavior can be expressed by the single complementarity condition [4, 5]:

$$\Lambda_{N_i} \geq 0; \quad \dot{g}_N^{(i)} \geq 0; \quad \Lambda_{N_i} \dot{g}_N^{(i)} = 0; \quad i \in \Omega_S^*. \tag{43}$$

The model (39) should be supplemented by Coulomb's friction law. The tangential impulse can be derived in a similar way as equation (40), by integration:

$$\Lambda_{Tl_i} = \lim_{t'_{c_i} \to t''_{c_i}} \int_{t'_{C_i}}^{t''_{C_i}} F_{Tl_i}\, dt; \quad \Lambda_{Tt_i} = \lim_{t'_{c_i} \to t''_{c_i}} \int_{t'_{c_i}}^{t''_{c_i}} F_{Tt_i}\, dt; \quad i \in \Omega_S^*. \tag{44}$$

Now, we state a tangential impact law in the longitudinal direction $g_{Tl}^{(i)}$ as [5]:

$$|\Lambda_{Tl_i}| \leq \mu_i \Lambda_{N_i}; \quad i \in \Omega_S^*$$
$$\begin{cases} |\Lambda_{Tl_i}| < \mu_i \Lambda_{N_i} & \Rightarrow \quad \dot{g}_{Tl}^{(i)} = 0 \quad stick \quad state \\ \Lambda_{Tl_i} = +\mu_i \Lambda_{N_i} & \Rightarrow \quad \dot{g}_{Tl}^{(i)} \leq 0 \quad slip \quad state \\ \Lambda_{Tl_i} = -\mu_i \Lambda_{N_i} & \Rightarrow \quad \dot{g}_{Tl}^{(i)} \geq 0 \quad slip \quad state \end{cases} \tag{45}$$

as well as in the transversal direction $g_{Tt}^{(i)}$:

$$|\Lambda_{Tt_i}| \leq \mu_i \Lambda_{N_i}; \quad i \in \Omega_S^*$$
$$\begin{cases} |\Lambda_{Tt_i}| < \mu_i \Lambda_{N_i} & \Rightarrow \quad \dot{g}_{Tt}^{(i)} = 0 \quad stick \quad state \\ \Lambda_{Tt_i} = +\mu_i \Lambda_{N_i} & \Rightarrow \quad \dot{g}_{Tt}^{(i)} \leq 0 \quad slip \quad state \\ \Lambda_{Tt_i} = -\mu_i \Lambda_{N_i} & \Rightarrow \quad \dot{g}_{Tt}^{(i)} \geq 0 \quad slip \quad state \end{cases} \tag{46}$$

Also, the dissipative character of equations (45) and (46) should be stressed out:

$$\Lambda_{Tl_i}\, \dot{g}_{Tl}^{(i)} \leq 0; \quad \Lambda_{Tt_i}\, \dot{g}_{Tt}^{(i)} \leq 0; \quad i \in \Omega_S^*. \tag{47}$$

Thus (45) and (46) should be regarded as independent tangential impact laws in two orthogonal tangential directions (longitudinal and transversal) which coincide with Coulomb's friction law [5] and contain all the main physical effects of dry friction. With (43), (45) and (46) the missing $3n_S^*$ impact conditions are found and the problem is closed in a mathematical sense, i.e. the number of unknows in the model (40) is equal to its order.

The dynamic equations (36), (45), (46), together with the corresponding kinematic relations (38) of the system, can be stated as an LCP formulation. Because of the system discontinuity (expressed by eqs. (45) and (46)), due to the non-smooth stick/slip characteristics, the LCP approach should be applied to both directions - the normal and the tangential. Initially, this demands decomposition of the friction characteristics (45) and (46), i.e. the decomposition of tangential characteristics according to [4, 5]. The basic idea for decomposing friction characteristic is to formulate each of the tangential constraints by two simultaneously appearing constraints. Each of them transfers only one part of it. Both constraints transmit the tangential force F_{Tl_i} (F_{Tt_i}) by splitting it into the portions $F_{Tl}^{(+)}$ and $F_{Tl}^{(-)}$ ($F_{Tt}^{(+)}$ and $F_{Tt}^{(-)}$) in the positive and negative tangential directions [5], respectively. Then, the state F_{Tl_i} (F_{Tt_i}) can be written in the folowing way:

$$\begin{aligned} F_{Tl_i} &= F_{Tl_i}^{(+)} - F_{Tl_i}^{(-)}, \quad i \in \Omega_{H_1} \\ F_{Tt_i} &= F_{Tt_i}^{(+)} - F_{Tt_i}^{(-)}, \quad i \in \Omega_{H_2} \end{aligned} \tag{48}$$

The values $F_{Tl}^{(+)}$ and $F_{Tl}^{(-)}$ ($F_{Tt}^{(+)}$ and $F_{Tt}^{(-)}$) are not arbitrary but must be chosen in such a manner that the tangential force F_{Tl_i} (F_{Tt_i}) always lies in the convex set $C_{Tl_i}(C_{Tt_i})$ defined in the following way. The admissible values of the tangential forces F_{Tl_i} and F_{Tt_i} form the convex sets $C_{Tl_i}$and C_{Tt_i} which are bounded by the values of the normal force [5]:

$$\begin{aligned} C_{Tl_i} &= \{F_{Tl_i} \mid -\mu_i F_{N_i} \le F_{Tl_i} \le +\mu F_{N_i}\} \\ C_{Tt_i} &= \{F_{Tt_i} \mid -\mu_i F_{N_i} \le F_{Tt_i} \le +\mu F_{N_i}\}, \ i \in \Omega_S \end{aligned} \tag{49}$$

If the tangential forces F_{Tl_i} and F_{Tt_i} are in the interior of the sets $C_{Tl_i}$and C_{Tt_i}, then the continual sticking appears in both directions (the longitudinal $\dot{g}_{Tl}^{(i)} = 0$, $\ddot{g}_{Tl}^{(i)} = 0$ and the transversal $\dot{g}_{Tt}^{(i)} = 0$, $\ddot{g}_{Tt}^{(i)} = 0$). Otherwise, the tangential forces F_{Tl_i} and F_{Tt_i} lie at the boundaries of C_{Tl_i} and C_{Tt_i} and allow transition to sliding by arbitrary values of $\ddot{g}_{Tl}^{(i)}$ and $\ddot{g}_{Tt}^{(i)}$ in the oposing directions. This can be ensured by restricting the values of $F_{Tl}^{(+)}$ and $F_{Tl}^{(-)}$ ($F_{Tt}^{(+)}$ and $F_{Tt}^{(-)}$) to

$$\begin{aligned} F_{Tl_i}^{(+)} \in C_{Tl_i}^{(+)} &= \left\{F_{Tl_i}^{(+)} \mid 0 \le F_{Tl_i}^{(+)} \le \mu_i F_{N_i}\right\}, \\ F_{Tl_i}^{(-)} \in C_{Tl_i}^{(-)} &= \left\{F_{Tl_i}^{(-)} \mid -\mu_i F_{N_i} \le F_{Tl_i}^{(-)} \le 0\right\}, \quad i \in \Omega_{H_1} \\ F_{Tt_i}^{(+)} \in C_{Tt_i}^{(+)} &= \left\{F_{Tt_i}^{(+)} \mid 0 \le F_{Tt_i}^{(+)} \le \mu_i F_{N_i}\right\}, \\ F_{Tt_i}^{(-)} \in C_{Tt_i}^{(-)} &= \left\{F_{Tt_i}^{(-)} \mid -\mu_i F_{N_i} \le F_{Tt_i}^{(-)} \le 0\right\}, \quad i \in \Omega_{H_2} \end{aligned} \tag{50}$$

For each of the new variables $F_{Tl}^{(+)}$ and $F_{Tl}^{(-)}$ ($F_{Tt}^{(+)}$ and $F_{Tt}^{(-)}$) the connections to the tangential relative acceleration $\ddot{g}_{Tl}^{(i)}$ ($\ddot{g}_{Tt}^{(i)}$) should be defined in order to bring the system to the LCP formulation. In Figure 3.1 the decomposition of the friction characteristic (the longitudinal commponent) is presented according to [5]. Similar graphs are obtained for the characteristic in the transversal direction but they are not depicted separately.

The decomposition shown in Figure 3.1 enables the LCP formulation by using the resulting inequlities and complementarity conditions, together with the dynamic

equations derived previously. Following the decomposition procedure shown in Figures 3.1c and 3.1d one obtains [5]:

$$\begin{aligned} \ddot{g}_{Tl_i} &= z_i^+ - \ddot{g}_{Tl_i}^- \\ \ddot{g}_{Tl_i} &= \ddot{g}_{Tl_i}^+ - z_i^- \\ & \qquad\qquad i \in \Omega_{H_1} \\ F_{Tl0_i}^{(+)} &= \mu_i F_{N_i} - F_{Tl_i}^{(-)} \\ F_{Tl0_i}^{(-)} &= \mu_i F_{N_i} - F_{Tl_i}^{(+)} \end{aligned} \tag{51}$$

Similar relations can also be written for the accelerations and tangential forces in the transversal direction. The physical meaning of the auxilary variables z_i^+ and z_i^- is obvious by this set of equations. They denote just the positive as well as the negative parts of accelerations, and they have been introduced merely for the reason of distinctition. From (51), the following equivalencies hold: $z_i^+ = \ddot{g}_{Tl_i}^+, \quad z_i^- = \ddot{g}_{Tl_i}^-$. The terms $F_{Tl0_i}^{(+)}$ and $F_{Tl0_i}^{(-)}$ are called friction saturations (in the longitudinal direction) and stand for the differences of the maximal transferable and actual tangential forces. When they vanish, a transition to sliding is possible. Finally, the complementarity conditions, that are presented in Figure 3.1d, can be defined in the following way:

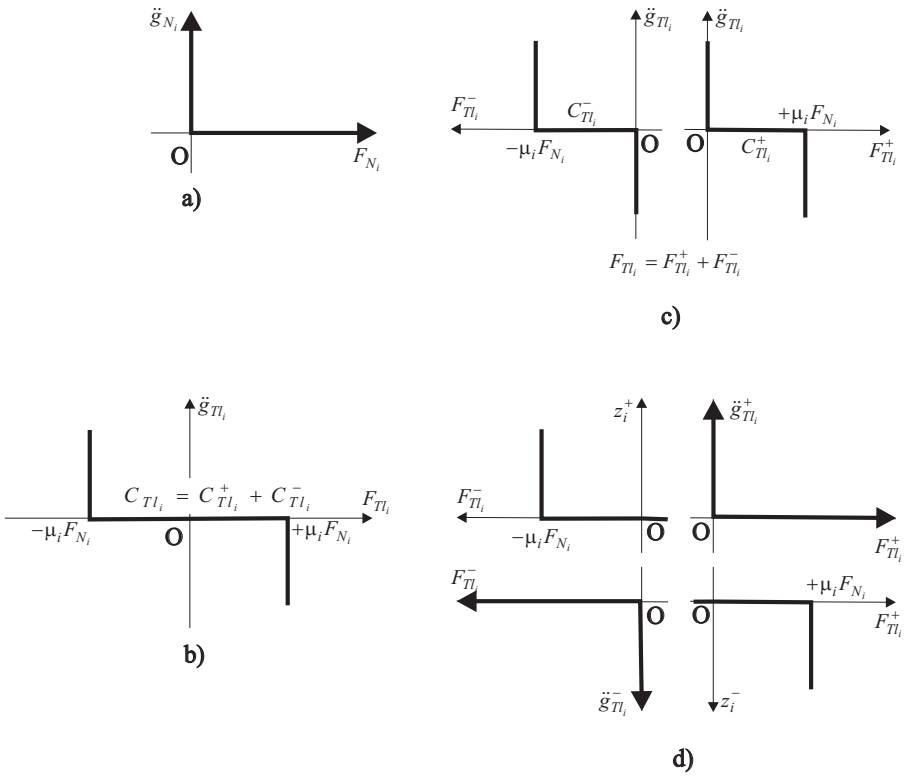

FIGURE 7. a) Complementarity of normal contacts; b) Friction characteristics during contact; c), d) Decomposition of the friction characteristic in two steps [5].

$$\begin{array}{lll} \ddot{g}_{Tl_i}^- \geq 0; & F_{Tl_i}^- \geq 0; & \ddot{g}_{Tl_i}^- F_{Tl_i}^- = 0 \\ \ddot{g}_{Tl_i}^+ \geq 0; & F_{Tl_i}^+ \geq 0; & \ddot{g}_{Tl_i}^+ F_{Tl_i}^+ = 0 \\ & & \qquad i \in \Omega_{H_1} \\ F_{Tl0_i}^+ \geq 0; & z_i^+ \geq 0; & F_{Tl0_i}^+ z_i^+ = 0 \\ F_{Tl0_i}^- \geq 0; & z_i^- \geq 0; & F_{Tl0_i}^- z_i^- = 0 \end{array} \tag{52}$$

The set of relations (52) describes in full the decomposed friction characteristics which correspond to four unilateral constraints. Equations (48)-(52) have to be used for each of the potentially sticking contacts $i \in \Omega_{H_1}$.

Now, the impact model is fully determined by the corresponding kinetics (36) and kinematics equation (38) of biped locomotion system, the impact law in the normal direction (43), and the tangential impact characteristics (45) and (46). In order to determine the model unknowns (the transferred impact impulses $\Lambda_N(t_c')$, $\Lambda_{Tl}(t_c')$, $\Lambda_{Tt}(t_c')$, as well as the impact velocities $\underline{\dot{g}}_N(t_c'')$, $\underline{\dot{g}}_{Tl}(t_c'')$, $\underline{\dot{g}}_{Tt}(t_c'')$) the LCP formulation will be applied [4, 5]. For that purpose, because of the non-smoothness and discontinuity of the friction dynamics, the decomposition of the tangential relative velocities $\underline{\dot{g}}_{Tl}(t_c'')$, $\underline{\dot{g}}_{Tt}(t_c'')$ and tangential impact impulses $\Lambda_{Tl}(t_c')$, $\Lambda_{Tt}(t_c')$ is performed in a way described by (48)-(52) [5]. Finally, the impact model of biped gait is defined in an LCP form. For establishing equations for the LCP, (48), (51) and (52) should be integrated over the impact interval $|deltat$. Then the following relations are obtained:

$$\begin{array}{lll} \Lambda_{Tl_i} = \Lambda_{Tl_i}^{(+)} - \Lambda_{Tl_i}^{(-)}, & i \in I_{H_1} & \\ \dot{g}_{Tl_i} = z_i^+ - \dot{g}_{Tl_i}^-; & \Lambda_{Tl0_i}^{(+)} = \Lambda_{G_i}^{(-)} - \Lambda_{Tl_i}^{(-)}; & i \in \Omega_{H_1} \\ \dot{g}_{Tl_i} = \dot{g}_{Tl_i}^+ - z_i^-; & \Lambda_{Tl0_i}^{(-)} = \Lambda_{G_i}^{(+)} - \Lambda_{Tl_i}^{(+)}; & \end{array} \tag{53}$$

and

$$\begin{array}{lll} \dot{g}_{Tl_i}^- \geq 0; & \Lambda_{Tl_i}^{(-)} \geq 0; & \dot{g}_{Tl_i}^- \Lambda_{Tl_i}^{(-)} = 0 \\ \dot{g}_{Tl_i}^+ \geq 0; & \Lambda_{Tl_i}^{(+)} \geq 0; & \dot{g}_{Tl_i}^+ \Lambda_{Tl_i}^{(+)} = 0 \\ & & \qquad i \in \Omega_{H_1} \\ \Lambda_{Tl0_i}^{(+)} \geq 0; & z_i^+ \geq 0; & \Lambda_{Tl0_i}^{(+)} z_i^+ = 0 \\ \Lambda_{Tl0_i}^{(-)} \geq 0; & z_i^- \geq 0; & \Lambda_{Tl0_i}^{(-)} z_i^- = 0 \end{array} \tag{54}$$

All tangential impulses Λ_{Tl} of the impact contacts $i \in \Omega_S^*$ can be defined as a vector difference:

$$\begin{array}{l} \Lambda_{Tl} = \Lambda_{Tl}^{(+)} - \Lambda_{Tl}^{(-)}; \\ \Lambda_{Tl}^{(+)} = \left[\Lambda_{Tl_1}^{(+)} \ \ldots \Lambda_{Tl_{n_S^*}}^{(+)}\right]^T; \quad \Lambda_{Tl}^{(-)} = \left[\Lambda_{Tl_1}^{(-)} \ \ldots \Lambda_{Tl_{n_S^*}}^{(-)}\right]^T \end{array} \tag{55}$$

Then, taking into account equations (36) and (38), the following LCP form of the relation can be derived:

$$\begin{array}{l} \begin{bmatrix} \underline{\dot{g}}_C \\ \Lambda_{T0_C} \end{bmatrix} = \begin{bmatrix} W_S^T H^{-1} W_S & I_S^T \\ N_S - I_S & \underline{0} \end{bmatrix} \cdot \begin{bmatrix} \Lambda_C \\ z_C \end{bmatrix} + \begin{bmatrix} \underline{\dot{g}}_A \\ \underline{0} \end{bmatrix} \\ \begin{bmatrix} \underline{\dot{g}}_C \\ \Lambda_{T0_C} \end{bmatrix} \geq \underline{0}; \quad \begin{bmatrix} \Lambda_C \\ z_C \end{bmatrix} \geq \underline{0}; \quad \begin{bmatrix} \underline{\dot{g}}_C \\ \Lambda_{T0_C} \end{bmatrix}^T \cdot \begin{bmatrix} \Lambda_C \\ z_C \end{bmatrix} = \underline{0}; \end{array} \tag{56}$$

where the matrices and vectors used have the forms:

$$\underline{\dot{g}}_C = \begin{bmatrix} \underline{\dot{g}}_N \\ +\underline{\dot{g}}_{Tl} \\ +\underline{\dot{g}}_{Tt} \\ -\underline{\dot{g}}_{Tl} \\ -\underline{\dot{g}}_{Tt} \end{bmatrix}; \quad \underline{\dot{g}}_A = \begin{bmatrix} \underline{\dot{g}}_N \\ \underline{\dot{g}}^+_{Tl} \\ \underline{\dot{g}}^+_{Tt} \\ \underline{\dot{g}}^-_{Tl} \\ \underline{\dot{g}}^-_{Tt} \end{bmatrix}; \; z_C = \begin{bmatrix} z^-_C \\ z^+_C \end{bmatrix} = \begin{bmatrix} \underline{\dot{g}}^-_{Tl} \\ \underline{\dot{g}}^-_{Tt} \\ \underline{\dot{g}}^+_{Tl} \\ \underline{\dot{g}}^+_{Tt} \end{bmatrix}; \; \Lambda_C = \begin{bmatrix} \Lambda_N \\ \Lambda^{(+)}_{Tl} \\ \Lambda^{(+)}_{Tt} \\ \Lambda^{(-)}_{Tl} \\ \Lambda^{(-)}_{Tt} \end{bmatrix};$$

$$W_S = \begin{bmatrix} W^T_N \\ +W^T_{Tl} \\ +W^T_{Tt} \\ -W^T_{Tl} \\ -W^T_{Tt} \end{bmatrix}; \quad I^T_S = \begin{bmatrix} \underline{0} & \underline{0} & \underline{0} & \underline{0} \\ E & \underline{0} & \underline{0} & \underline{0} \\ \underline{0} & E & \underline{0} & \underline{0} \\ \underline{0} & \underline{0} & E & \underline{0} \\ \underline{0} & \underline{0} & \underline{0} & E \end{bmatrix}; \tag{57}$$

$$N_S - I_S = \begin{bmatrix} \overline{\mu}_S & -E & \underline{0} & \underline{0} & \underline{0} \\ \overline{\mu}_S & \underline{0} & -E & \underline{0} & \underline{0} \\ \overline{\mu}_S & \underline{0} & \underline{0} & -E & \underline{0} \\ \overline{\mu}_S & \underline{0} & \underline{0} & \underline{0} & -E \end{bmatrix};$$

$$\Lambda_{T0_C} = \begin{bmatrix} \Lambda^{(-)}_{Tl0} \\ \Lambda^{(-)}_{Tt0} \\ \Lambda^{(+)}_{Tl0} \\ \Lambda^{(+)}_{Tt0} \end{bmatrix} = \begin{bmatrix} \Lambda^{(-)}_{T0_C} \\ \Lambda^{(+)}_{T0_C} \end{bmatrix} = (N_S - I_S) \cdot \Lambda_C$$

$E \in \mathbb{R}^{n^*_S \times n^*_S}$ is a unit matix and $\overline{\mu}_S \in \mathbb{R}^{n^*_S \times n^*_S}$ is a diagonal matrix consisting of the coefficients of friction μ_i. Dimensions of the vectors and matrices used in (56) are: $\dot{g}_N, \dot{g}_A, \Lambda_C \in \mathbb{R}^{5n^*_S \times 1}$, $W_S \in \mathbb{R}^{N \times 5n^*_S}$, $\Lambda_{T0_C}, z_C \in \mathbb{R}^{4n^*_S \times 1}$.

Relation (56) represents the standard LCP formulation of the impact law that can be written in a general form:

$$\begin{array}{l} y = A\,x + b; \quad y \geq \underline{0}; \quad x \geq \underline{0}; \quad y^T x = \underline{0} \\ y,\; x \in R^{5\,n_s} \end{array} \tag{58}$$

Its solution $y \in \mathbb{R}^{5n_S}$, $x \in \mathbb{R}^{5n_S}$ contains all unkonown contact impulses and velocities during the impact. Lemke's algorithm [8] is here used to solve can be used (58). This robust algorithm ensures at least the existence of solution.

4. **Modeling of foot contact using the impedance model.** The impedance model presented in this section is usually implemented to describe the foot contact during the biped locomotion .

Generally, under the notion "robotic dynamic environment" it can be assumed both the ground support on which the locomotion mechanism moves and elastic footpad of the supporting leg. During the walk, the interactive forces and moments of dynamic environment reaction are transferred onto the entire mechanism structure. The 3D-model of environment used in our numerical simulation examples is presented in Figure 4. It can be considered as a spring-mass-damper mechanic system, while the model of dynamic environment is assumed to be composed of rigid ground support and elastic footpads. The impedance model, presented here, consisting of four vertical units of a linear spring and a non-linear damper at the corners $i = 1, ..., 4$ (4) was elaborated in [9]. The two pairs of horizontal units consisting of a linear spring and a linear damper at the heel and toes, aligned along

the walking and lateral directions, are also included in the 6-DOF model (Figure 4).. The nonlinear vertical springs prevent the elastic pad from being sqeezed more than is its thickness. The nonlinear damper model is used to describe accurately the impacts at the foot landing, as suggested in . The inertia effects, taking into account the engaged mass of the footpad, are included in the model, too. Note also that this model of elastic pad also allows its rotational deformation due to the moment applied at the foot, as well as its asymmetric vertical deformation. As a result, it is possible for the foot in contact with the ground to move and rotate in any direction.

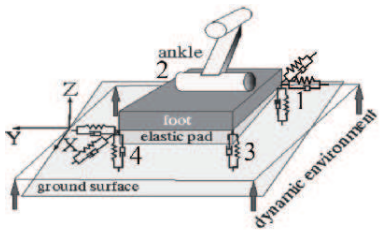

FIGURE 8. Impedance model of a foot contact.

The resultant vertical reaction force F_z generated at the foot in contact with the ground can be determined from the following relations:

$$F_z = \sum_{i=1}^{4} F_{z_i} \tag{59}$$

where

$$F_{z_i} = \begin{cases} m_i(\delta_i)\ddot{\delta_i} + k_z(\delta_i)\delta_i(\frac{3}{2}\alpha\dot{\delta_i} + 1), & \text{when } \dot{\delta_i} > 0, \delta_i > 0 \\ k_z(\delta_i)\delta_i & \text{when } \dot{\delta_i} < 0, \delta_i > 0 \\ 0 & \text{otherwise.} \end{cases} \tag{60}$$

where δ_i is the amount of deformation at the corner of the elastic pad (Figure 4), α is a constant which defines the relation between the coefficient of restitution and the impact velocity, t_p is the thickness of the elastic pad, $m_i = m_0\frac{\delta_i}{4t_p}$ is the engaged/compressed mass of the elastic pad and $k_z(\delta_i)$ is the stiffness associated with the spring model of the pad in the vertical direction defined by

$$k_z(\delta_i) = k_{z0}[1 + 0.1tan^3(\frac{\pi(\delta_i)}{2t_p})], \quad \text{for } 0 < \delta_i < t_p$$

and Note that the damping force generated at the corner i of the elastic pad becomes zero when $\dot{\delta_i} < 0$ and $\delta_i > 0$. Under the assumption that the elastic pad is in contact with the ground at the pad location i, the horizontal forces F_x and F_y generated by the elastic pad are represented by:

$$F_x = \sum_{i=1}^{4} F_{x_i} \tag{61}$$

where

$$F_{x_i} = \begin{cases} -m_i\ddot{x_i} - b_{xi}\dot{x_i} - k_{xi}(x_i - x_{0i}) & \text{stick state} \\ -\mu_{xi}F_{y_i}sign(\dot{x_i}) & \text{slip state.} \end{cases} \tag{62}$$

and

$$F_y = \sum_{i=1}^{4} F_{y_i} \tag{63}$$

where

$$F_{y_i} = \begin{cases} -m_i\ddot{y}_i - b_{yi}\dot{y}_i - k_{yi}(y_i - y_{0i}) & \text{case of stick friction} \\ -\mu_{yi}F_{y_i}sign(\dot{y}_i) & \text{case of slip.} \end{cases} \tag{64}$$

where $\dot{x}_i$ and $\dot{y}_i$ are displacement rates of the corner i of the footpad in the $x-$ and $y-$directions; x_{0i} and y_{0i} are the horizontal foot positions used to compute the horizontal forces due to the horizontal deformations of the elastic pad. They are defined as the positions of pad location i at the moment of the initial pad contact with the ground; $x_i - x_{0i}$ and $y_i - y_{0i}$ are the corresponding elastic deformations of the footpad in the observed directions; k_{xi} and k_{yi} are the stiffnesses associated with the spring model of the pad in the horizontal directions at the location i; b_{xi} and b_{yi} represent the damping associated with the model of the pad in the horizontal directions at the location i; μ_{xi} and μ_{yi} are Coulomb friction coefficients in the horizontal directions. The stick state exists in the quasi-static case when the foot displacement rate is small or equal to zero. Then, only the elastic deformation of elastic pad appears in the contact area. Coulomb friction appears as a consequence of the foot slippage over the supporting surface.

Ground reaction moments of the robot foot can be determined from the following relations:

$$M_x = (F_{z_1} + F_{z_3} - F_{z_2} - F_{z_4})\frac{w_p}{2} \tag{65}$$

$$M_y = (-F_{z_1} + F_{z_3} - F_{z_2} + F_{z_4})\frac{l_p}{2} \tag{66}$$

$$M_z = -(F_{z_1} + F_{z_4})\frac{\omega_p}{2} + F_{y_1} - F_{y_4})\frac{l_p}{2} \tag{67}$$

where w_p are l_p the width and length of the elastic pad.

5. **Results and comments.** Two contact models (LCP formulation and impedance model) have been implemented. The simulations have been performed under the same conditions. Note that for the simulation of the kinematic and dynamic models follow the lines of [10]. A forward velocity $v = 1m/s$, a step seize $s = 0.75m$ and an average lifting height of the robot foot $h = 0.15m$ were introduced. For control of the dynamically balanced biped gait of robot mechanism, the impedance control with the complementarity ZMP compensator is used [11]. The structure as well as the control parameters used in simulation experiments are same for both simulation tests. In order to validate simulation results, the corresponding experiments have been performed using a VICON caption motion studio equipment with the appropriate software package [12] for processing measurement data. Monitoring of the position markers during the motion was performed using six VICON high-accuracy infra-red cameras with the recording frequency of 200 $[Hz]$. Reactive forces of the foot impact/contact with the ground were measured on the force platform with a recording frequency of 1.0 $[Ghz]$.

Both models of contact/impact forces applied in the simulation experiments show good similarity with experimental measurements (presented in Figures 9 and 2) performed in the capture motion studio. Foot sole cycloids obtained for both models

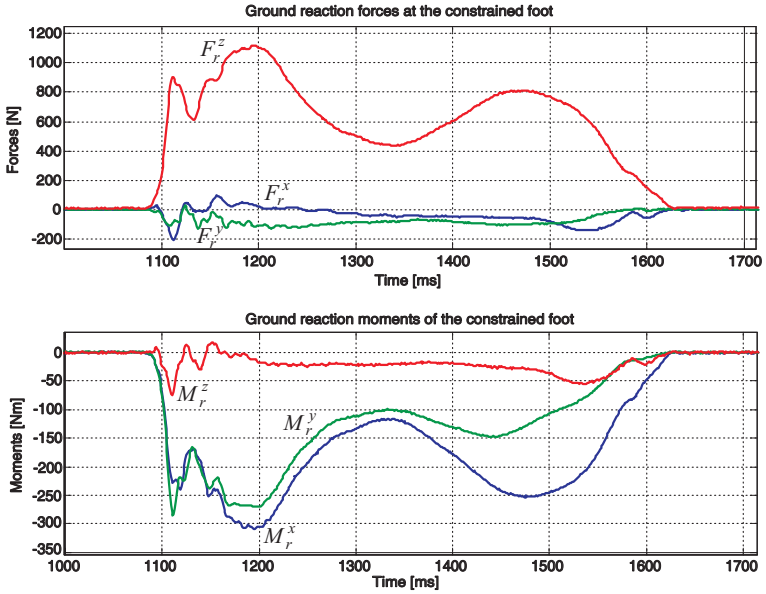

FIGURE 9. Experimentally measured ground reaction forces and moments on a single foot of the subject under laboratory conditions.

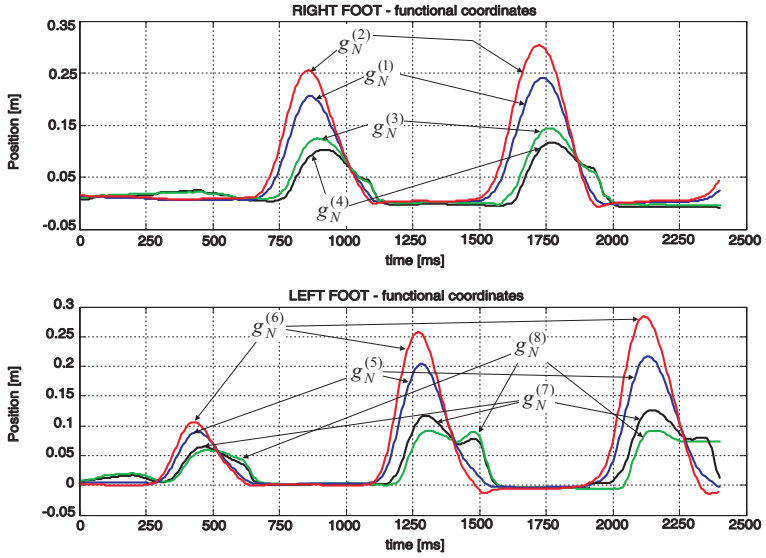

FIGURE 10. Functional coordinates $g_N^{(i)}$ determining the relative positions of the right and left feet contour points $i = 1, \ldots, 8$ with respect to the support in the normal direction.

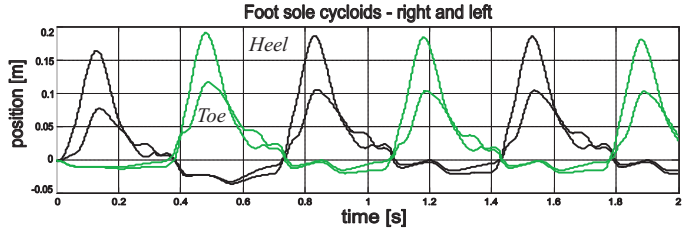

a)

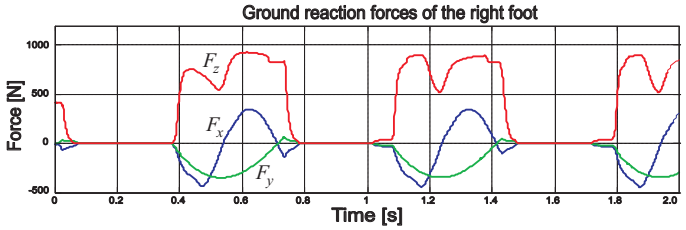

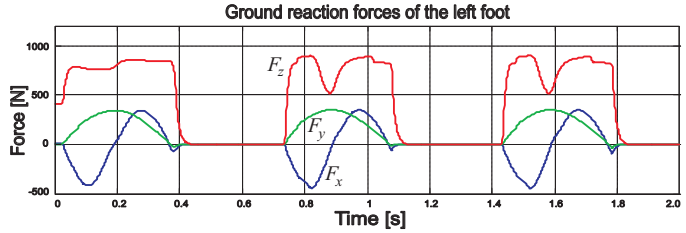

b)

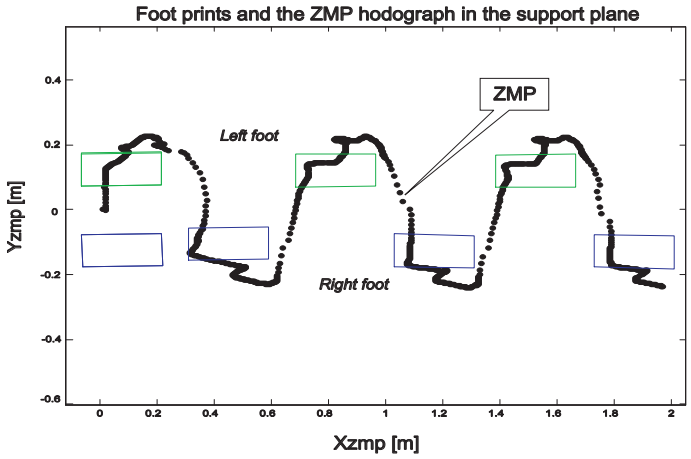

c)

FIGURE 11. Simulation results obtained for the use of the LCP model of contact dynamics: a) feet cycloids, b) ground reaction forces in the sagital Fx, lateral Fy and vertical direction Fz, c) ZMP hodograph.

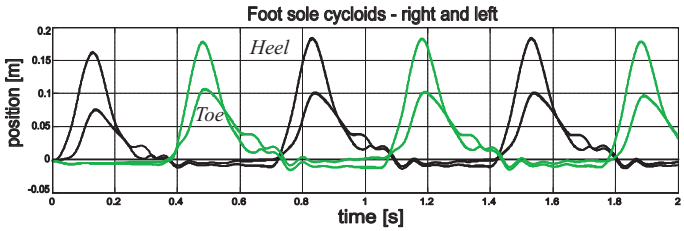

a)

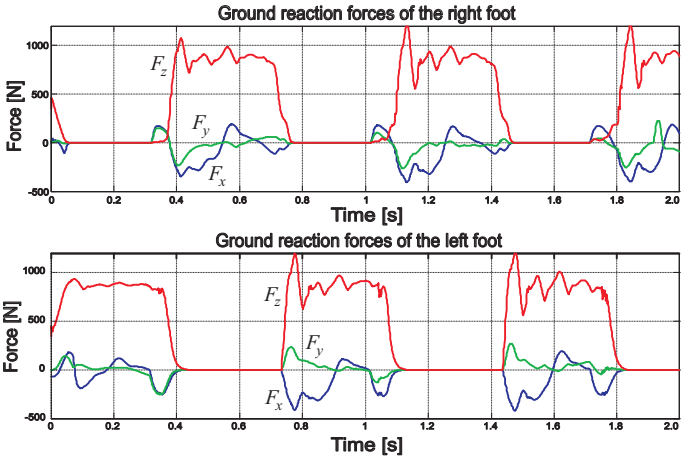

b)

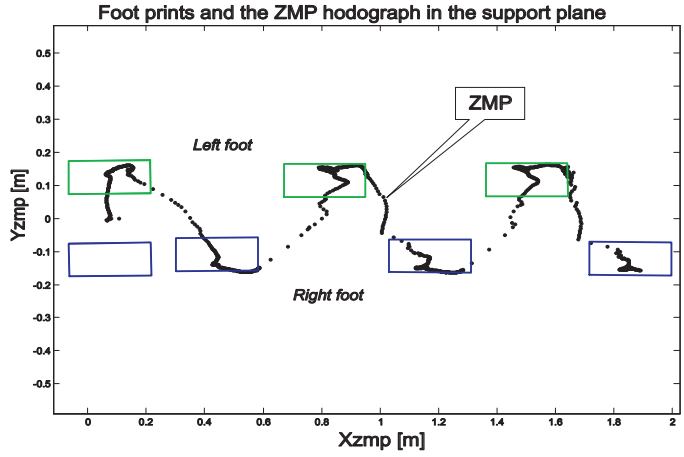

c)

FIGURE 12. Simulation results obtained for the use of the impedance model of contact dynamics: a) feet cycloids, b) ground reaction forces in the sagital Fx, lateral Fy and vertical direction Fz, c) ZMP hodograph.

considered are presented in Figures 11a and 12a. It is evident that impedance model of foot-ground contact reactions takes into account the real deformations of the supporting surface due to its elasticity (Fig. 12a). In this case it is just few millimeters.

Corresponding ground reaction forces are shown in Figures 11b and 12b. LCP model ensures better smoothness of the reactive forces (Figure 11b) while impedance model takes into account dynamics of the environment (supporting surface) and because of that the obtained forces have certain variations of the amplitudes.

ZMP hodographs in both simulation cases track the trajectories of the biped feet, i.e. corresponding dynamics of the imposed biped gait (Figures 11c and 12c). In order to maintain the dynamic balance of the biped, the ZMP always stays inside the supporting polygone.

The impact modelling based on LCP formulation (and variational inequalities in general) is more accurate for non-smooth multi-point impact/contact dynamics of biped gait and analysis of system stability. The implemented formulation has at least one solution [13] and the Lemke's algorithm is suitable for the numerical implementation. In the other hand, this formulation is more theoretical and requires from the engineering community more mathematical background especially the numerical implementation is quite technical.

The impedance model is rather more practical and oriented towards satisfying engineering aspects of solving impact problems for engineering problems.

Acknowledgments. The authors are indebted to Professor Georges Dalleau, Laboratory of Biomechanics, University of La Réunion, France, for his help in performing experimental measurements. Authors express their gratitude to the Alexander von Humboldt Foundation, Germany and to the PHC Pavle Savic French-Serbian bilateral program that partly support this research project.

REFERENCES

[1] V. Potkonjak and M. Vukobratovic, *A generalized approach to modeling dynamics of human and humanoid motion*, International Journal of Humanoid Robotics, **2** (2005), 21–45.

[2] A. Rodic and M. Vukobratovic, *Contribution to the integrated control of biped locomotion mechanisms*, International Journal of Humanoid Robotics, **4** (2007), 49–95.

[3] K. Addi and M. Cadivel, *A study of dynamical system involving monotone and nonmonotone constraints: The regularized-penalized problem*, Advances in Nonlinear Variational Inequalities, **7** (2004), 1–33.

[4] B. Brogliato, "Nonlinear Impact Mechanics: Models, Dynamics and Control," Springer-Verlag, London, 1996.

[5] F. Pfeiffer and Ch. Glocker, "Multibody Dynamics with Unilateral Contacts," Wiley Series in Nonlinear Science. A Wiley-Interscience Publication, John Wiley & Sons, Inc., New York, 1996.

[6] A. Rodic, M. Vukobratovic, K. Addi and G. Dalleau, *Contribution to the modeling of non-smooth, multi-point contact dynamics of biped locomotion - theory and experiments*, Robotica, **26** (2008), 157–175.

[7] M. Vukobratovic, B. Borovac, D. Surla and D. Stokic, "Biped Locomotion: Dynamics, Stability, Control and Application," Springer-Verlag, 1989.

[8] C. A. Lemke, *Some pivot scheme for the linear complementarity problem*, Complementarity and fixed point problems. Math. Programming Stud. No. 7, (1978), 15–35.

[9] J. H. Park, *Impedance control for biped robot locomotion*, IEEE Transactions on Robotics and Automation, **17** (2001), 870–882.

[10] R. P. Paul, "Robot Manipulators: Mathematics, Programming, and Control," The MIT Press, Cambridge, Massachustets & London, England, 1981.

[11] A. Rodic, K. Addi and G. Dalleau, "Adaptive Bio-inspired Control of Humanoid Robots From Human Locomotion to Artificial Biped Gait of High Performences," Chapter in the book Contemporary Robotics - Challenges and Solutions, In-Tech, ISBN-978-953-307-038-4, pp. 275-300, 2009.
[12] A. Rodic, "Customized Software Interface for Enhanced 3D-Sensing, Modeling and Simulation of Human Biomechanics for Use with Marker-Based Capture Motion Systems," on-line available at http://www.institutepupin.com/RnDProfile/ROBOTIKA/capmot.htm
[13] R. W. Cottle, J. S. Pang and R. E. Stone, "The Linear Complementarity Problem," Computer Science and Scientific Computing, Academic Press, Inc., Boston, MA, 1992.

Received September 8, 2009; Accepted December 23, 2009.

E-mail address: khalid.addi@univ-reunion.fr
E-mail address: roda@robot.imp.bg.ac.yu